

WestminsterResearch

<http://www.westminster.ac.uk/westminsterresearch>

**Automated Measurement of Pancreatic Fat and Iron
Concentration Using Multi-Echo and T1-Weighted MRI Data**

**Basty, N., Liu, Y., Cule, M., Thomas, E.L., Bell, J.D. and Whitcher,
B.**

This is a copy of the author's accepted version of a paper subsequently published in the proceedings of the International Symposium on Biomedical Imaging 2020, Iowa City, USA 03 - 07 Apr 2020.

The final published version is available online at:

<https://doi.org/10.1109/ISBI45749.2020.9098650>

© 2020 IEEE . Personal use of this material is permitted. Permission from IEEE must be obtained for all other uses, in any current or future media, including reprinting/republishing this material for advertising or promotional purposes, creating new collective works, for resale or redistribution to servers or lists, or reuse of any copyrighted component of this work in other works.

The WestminsterResearch online digital archive at the University of Westminster aims to make the research output of the University available to a wider audience. Copyright and Moral Rights remain with the authors and/or copyright owners.

AUTOMATED MEASUREMENT OF PANCREATIC FAT AND IRON CONCENTRATION USING MULTI-ECHO AND T1-WEIGHTED MRI DATA

Nicolas Bastyl¹, Yi Liu², Madeleine Cule², E. Louise Thomas¹, Jimmy D. Bell¹, Brandon Whitcher¹

¹Research Centre for Optimal Health, School of Life Sciences, University of Westminster, London, United Kingdom

²Calico Life Sciences LLC, South San Francisco, United States

ABSTRACT

We present an automated method for estimation of proton density fat fraction and iron concentration in the pancreas using both structural and quantitative imaging data present in the UK Biobank abdominal MRI acquisition protocol. Our method relies on automatic segmentation of 3D T1-weighted MRI data using a convolutional neural network and extracting the location of the multi-echo slice through the segmented volume. We finally estimate the fat and iron content in the pancreas using the extracted segmentation as a mask on the multi-echo data. Our segmentation model achieves a mean dice similarity coefficient of 0.842 ± 0.071 on unseen data, which is comparable to the current state of the art for 3D segmentation of the pancreas. The proposed method is efficient and robust and enables an enhanced analysis of spatial distribution of proton density fat fraction and iron concentration over the current practice of manually placing regions of interest on often ambiguous multi-echo data.

Index Terms— Pancreas, MRI, UK Biobank, Fat, Iron

1. INTRODUCTION

The pancreas plays a fundamental role in the overall homeostasis of the body and its dysfunction has been closely associated with a number of important clinical conditions. Pancreatic fat accumulation and changes in iron levels have recently become important indicators of conditions including type 2 diabetes and pancreatic cancer, which has led to growing research interest focusing on non-invasive accurate estimation of proton density fat fraction (PDFF) and iron concentration of the pancreas using multi-echo MRI [1- 3].

Two of the UK Biobank MRI protocols for abdominal acquisitions focus on the pancreas. Every participant undergoes a 3D T1-weighted (T1w) as well as a single-slice

multi-echo acquisition. Together they enable accurate structural and quantitative analysis of the pancreas. Multi-echo MRI is a quantitative MRI pulse sequence enabling accurate non-invasive estimation of tissue composition elements including PDFF and iron concentration. However, this sequence suffers from poor anatomical quality and being restricted to a single two-dimensional slice through the abdomen. In addition to the poor visual quality of the multi-echo data, the irregular shape of the pancreas, anatomical position and often ambiguous boundaries results in large inter-subject variability of the cross-sectional area of the pancreas captured by the imaging plane of the multi-echo 2D acquisition. While manually segmenting the healthy pancreas from a multi-echo slice is challenging, it becomes almost impossible in an unhealthy one.

Current practice for non-invasive estimation of PDFF and iron concentration from multi-echo MRI involves practitioners manually placing regions of interest (ROIs) on the 2D data [4-8]. Manual placement is not only time consuming, but may also lead to increased variability in the parameter estimates due to ROI placement and the limited anatomical coverage. Both of these factors may have a substantial impact on the reproducibility of the measurements of PDFF and iron concentration as well as on the assessment of potential regional variation across the pancreas. While the multi-echo acquisition aims to contain as much of the pancreas as possible, its irregular shape may lead to the 2D image cutting through it more than once, resulting in several separate structures, further complicating manual annotation given the lack of 3D context. The need for an automated, robust and efficient method for organ segmentation and quantification is essential when working with large-scale data sets such as the UK Biobank, currently at ~45,000 participants with a final target of 100,000.

With the increasing availability of labeled medical data and more affordable computing power, convolutional neural

networks (CNNs) have become the standard solution for image processing tasks such as segmentation. Once trained, CNNs are able to produce segmentations in almost real time, a popular feature for large-scale data analysis. The first implementation of CNNs for segmentation of the pancreas was proposed by Roth et al. [10] for computed tomography (CT) acquisitions. This coarse-to-fine method, relying on a combination of superpixels, random forest classification, and a CNN, achieves a mean dice similarity coefficient (DSC) of 0.68 ± 0.1 . While MRI has the advantage of being non-ionizing, CT acquisitions are faster, have higher resolution and less ambiguous organ boundaries. CNNs have first been applied to pancreas segmentation from MRI data by Cai et al. [11], in which the authors make use of one network to classify pancreatic tissue and another to detect boundaries, giving a DSC of 0.761 ± 0.087 . The above methods segment on a slice by slice basis, meaning the loss of spatial out of plane context. This is expanded in [12], where recurrent networks are used to refine the consistency of the shape between adjacent slices, leading to an improved DSC of 0.802 ± 0.079 . Recent work by Asaturyan et al. [13], not based on CNNs but rather on geometrical descriptors, achieves a DSC of 0.815 ± 0.051 . In [14], the authors expand their methods to include CNNs, getting DSC of 0.841 ± 0.046 and 0.857 ± 0.023 on two different MRI datasets. To the best of our knowledge, the method proposed here is the first to have implemented CNNs with a full 3D volume input and output for pancreatic segmentation of MRI data.

The visual quality and non-standard coverage of the pancreas in multi-echo slices are challenges to overcome for segmentation of multi-echo data. For this, we propose a three-stage solution, exploiting T1w data for its structural information and multi-echo data for its quantitative information. Segmenting the image as opposed to being limited to ROIs enables an interrogation of spatial distribution of PDFF and iron concentration values.

2. METHODS

To overcome the issues associated with the single-slice multi-echo acquisition, we utilise the 3D T1w data available in the UK Biobank. We propose a three-step methodology for completely automated extraction of pancreatic PDFF and iron concentration. In the first step, a 3D segmentation is generated from the T1w volume, in the second step a slice of the segmented volume is extracted at the equivalent position to the coverage of the multi-echo imaging plane, see figure 1, in order to effectively segment the 2D image. In the third step PDFF and iron concentration values are

extracted using the segmentation and the processed multi-echo data.

For the 3D segmentation task, we trained a V-net [9]. The V-net architecture makes use of residual learning, learning parametric activation functions and 3D convolutional layers which have made it a strong candidate for volumetric segmentation. We reduced the number of filters in every convolutional layer by a factor of two, producing a more efficient model. Ninety-eight 3D T1w MRI acquisitions were manually annotated by a dedicated radiographer to produce the ground truth labels. The subjects were randomly selected from a subgroup of 1000 that were carefully chosen to cover a broad range of age, BMI, and sex. The data were split into 68 training and 30 test samples. The training data was normalised and augmented by a factor of 10 using minor translations of at most four voxels in all three dimensions. Note, flips or rotations were not applied as these operations have shown to cause a reduction in our model performance. This may be due to the regularity of the data, where the subjects are consistently placed in the same position and orientation inside the scanner. The model was trained to minimise a DSC loss over 185 epochs needed for convergence using a learning rate of $1e-5$ and a batch size of 1 on a NVIDIA Titan V 12 GB GPU which took 39 hours.

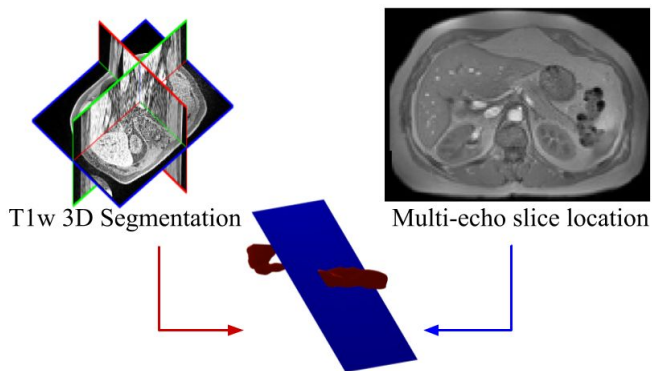


Figure 1 - Schematic of the method showing the combination of T1w 3D organ segmentation and the slice location of the multi-echo 2D image.

Post-processing was applied to the segmented pancreas volumes including binarising the network output by thresholding non-zero values, erosion of two voxels to ensure the final segmented object did not suffer from partial volume effects or include voxels from tissue other than the pancreas. Non-contiguous voxels unconnected to the largest segmented object (pancreas) were discarded. Estimates of the pancreas PDFF and iron concentration were obtained for each subject by extracting a 2D segmentation mask from the

network output by using the meta information from the single-slice multi-echo image to extract a slice from the segmented 3D T1w volume at the equivalent location [15]. Slice extraction makes the assumption that the 2D slice and the 3D volume overlap and do not suffer from major misalignment.

PDFF and R2* values from the multi-echo data were estimated on a pixel-by-pixel basis applying the methods described by Bydder et al. in [16]. Iron concentration was estimated using the formula defined by Wood et al. [4], using the R2* values obtained in the PDFF calculation.

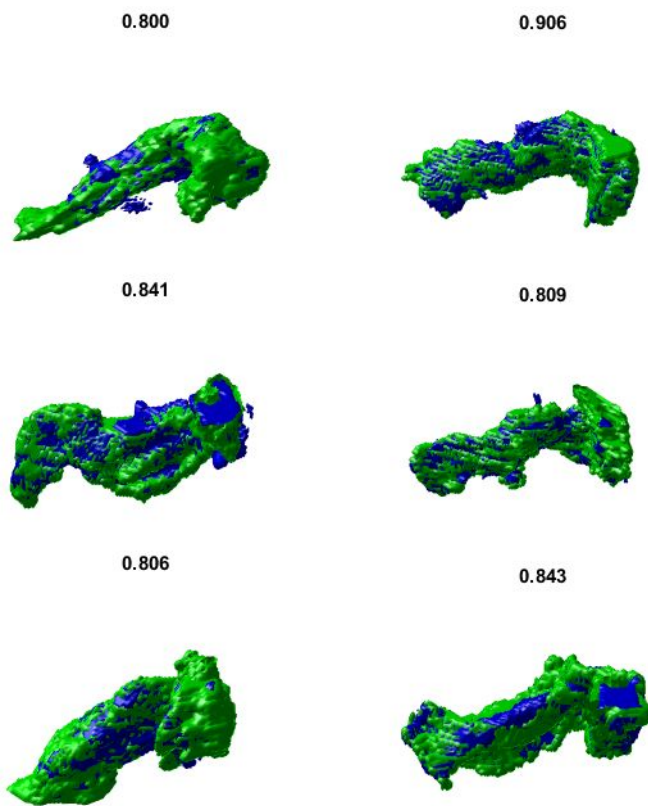


Figure 2 - Surface renderings of ground-truth (green) and CNN segmentations (blue) for six of the 3D T1w test datasets. The DSC for each segmentation is indicated above.

3. RESULTS

The segmentation model achieves a DSC of 0.842 ± 0.071 on unseen test data. The DSCs were calculated prior to the erosion but after discarding unconnected voxels of the network output. All of the figures we show in this section contain unseen test data. A comparison of manual segmentations and segmentations produced by the model before applying erosion may be found in figure 2. Figure 3

shows a multi-echo image on its own, showcasing the difficulty of the ROI placement task, as well as the corresponding segmentations extracted from the CNN segmentation (red) and from the ground truth volume (green) and their overlap (yellow) superimposed on the multi-echo slice. Histograms of the extracted PDFF and iron median values for the test data are shown in figure 4.

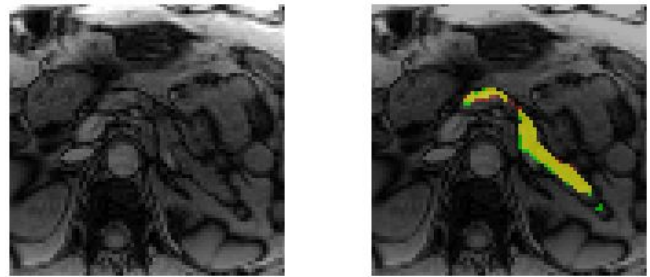


Figure 3 - Left: Multi-echo slice. Right: superimposed CNN segmentation (red), ground truth (green), overlap (yellow).

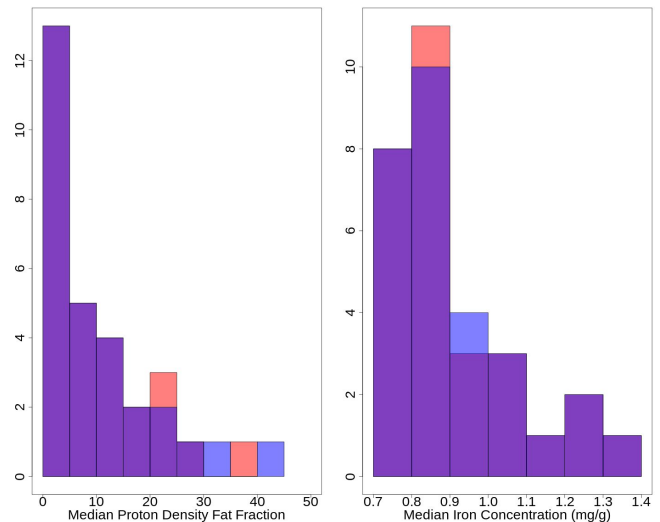


Figure 4 - Histograms of median PDFF (left) and iron concentration (right) for 30 test subjects. Red: segmentations extracted from CNN output, blue: segmentations extracted from manual segmentations, purple: overlap.

4. DISCUSSION & CONCLUSIONS

We have proposed and implemented a method for efficient, automated extraction of PDFF and iron concentration values using 3D T1w MRI as well as 2D multi-echo MRI pancreatic acquisitions that makes manual ROI placement obsolete. With a DSC of 0.842 ± 0.071 , our 3D segmentation

model achieves a similar performance to the best performing methods for segmentation of the pancreas in MRI data, such as 0.802 ± 0.079 by Cai et al. [12] or 0.857 ± 0.023 by Asaturyan et al. [14]. Comparing the proposed method to extracting segmentations from the manual ground truth volumes, there is very good agreement between the segmentations in figure 3 and there are only minor differences in the results in figure 4.

Future work to improve the method, aiming to minimise the differences present in figures 3 and 4, will include tweaking the segmentation model by increasing the batch size to enable batch normalisation, additional data augmentation, using the entire data for training, as well as applying 2D-to-3D registration to the slice extraction step. The anatomical coverage achieved by segmenting the organ, as opposed to placing small ROIs, opens up the possibility for more sophisticated analyses, such as regional variation in PDFF and iron concentration distribution.

5. ACKNOWLEDGMENTS

This research has been conducted using the UK Biobank Resource under project 44584 and was funded by Calico Life Sciences LLC.

6. REFERENCES

- [1] Sakai, N.S., Taylor, S.A. and Chouhan, M.D., 2018. Obesity, metabolic disease and the pancreas—Quantitative imaging of pancreatic fat. *The British journal of radiology*, 91(1089), p.20180267.
- [2] Lingvay, I., Esser, V., Legendre, J.L., Price, A.L., Wertz, K.M., Adams-Huet, B., Zhang, S., Unger, R.H. and Szczepaniak, L.S., 2009. Noninvasive quantification of pancreatic fat in humans. *The Journal of Clinical Endocrinology & Metabolism*, 94(10), pp.4070-4076.
- [3] Wood, J.C., 2011. Impact of iron assessment by MRI. *ASH Education Program Book*, 2011(1), pp.443-450.
- [4] Wood, J.C., Enriquez, C., Ghugre, N., Tyzka, J.M., Carson, S., Nelson, M.D. and Coates, T.D., 2005. MRI R2 and R2* mapping accurately estimates hepatic iron concentration in transfusion-dependent thalassemia and sickle cell disease patients. *Blood*, 106(4), pp.1460-1465.
- [5] McKay, A., Wilman, H.R., Dennis, A., Kelly, M., Gyngell, M.L., Neubauer, S., Bell, J.D., Banerjee, R. and Thomas, E.L., 2018. Measurement of liver iron by magnetic resonance imaging in the UK Biobank population. *PLoS one*, 13(12), p.e0209340.
- [6] Heber, S.D., Hetterich, H., Lorbeer, R., Bayerl, C., Machann, J., Auweter, S., Storz, C., Schlett, C.L., Nikolaou, K., Reiser, M. and Peters, A., 2017. Pancreatic fat content by magnetic resonance imaging in subjects with prediabetes, diabetes, and controls from a general population without cardiovascular disease. *PLoS One*, 12(5), p.e0177154.
- [7] Chen, Y., Long, L., Jiang, Z., Zhang, L., Zhong, D. and Huang, X., 2019. Quantification of pancreatic proton density fat fraction in diabetic pigs using MR imaging and IDEAL-IQ sequence. *BMC medical imaging*, 19(1), p.38.
- [8] Hu, H.H., Kim, H.W., Nayak, K.S. and Goran, M.I., 2010. Comparison of fat-water MRI and single-voxel MRS in the assessment of hepatic and pancreatic fat fractions in humans. *Obesity*, 18(4), pp.841-847.
- [9] Milletari, F., Navab, N. and Ahmadi, S.A., 2016, October. V-net: Fully convolutional neural networks for volumetric medical image segmentation. In *2016 Fourth International Conference on 3D Vision (3DV)* (pp. 565-571). IEEE.
- [10] Roth, H.R., Lu, L., Farag, A., Shin, H.C., Liu, J., Turkbey, E.B. and Summers, R.M., 2015, October. Deeporgan: Multi-level deep convolutional networks for automated pancreas segmentation. In *International conference on medical image computing and computer-assisted intervention* (pp. 556-564). Springer, Cham.
- [11] Cai, J., Lu, L., Zhang, Z., Xing, F., Yang, L. and Yin, Q., 2016, October. Pancreas segmentation in MRI using graph-based decision fusion on convolutional neural networks. In *International Conference on Medical Image Computing and Computer-Assisted Intervention* (pp. 442-450). Springer, Cham.
- [12] Cai, J., Lu, L., Xing, F. and Yang, L., 2018. Pancreas segmentation in CT and MRI images via domain specific network designing and recurrent neural contextual learning. *arXiv preprint arXiv:1803.11303*.
- [13] Asaturyan, H., Gligorievski, A. and Villarini, B., 2019. Morphological and multi-level geometrical descriptor analysis in CT and MRI volumes for automatic pancreas segmentation. *Computerized Medical Imaging and Graphics*, 75, pp.1-13.
- [14] Asaturyan, H., Thomas, E.L., Fitzpatrick, J., Bell, J.D. and Villarini, B., 2019, October. Advancing Pancreas Segmentation in Multi-protocol MRI Volumes Using Hausdorff-Sine Loss Function. In *International Workshop on Machine Learning in Medical Imaging* (pp. 27-35). Springer, Cham.
- [15] Bastý, N., McClymont, D., Teh, I., Schneider, J.E. and Grau, V., 2017. Reconstruction of 3D Cardiac MR Images from 2D Slices Using Directional Total Variation. In *Molecular Imaging, Reconstruction and Analysis of Moving Body Organs, and Stroke Imaging and Treatment* (pp. 127-135). Springer, Cham.
- [16] Bydder, M., Yokoo, T., Hamilton, G., Middleton, M.S., Chavez, A.D., Schwimmer, J.B., Lavine, J.E. and Sirlin, C.B., 2008. Relaxation effects in the quantification of fat using gradient echo imaging. *Magnetic resonance imaging*, 26(3), pp.347-359.